INFECTION AND IMMUNITY, Sept. 2004, p. 4985–4995 Vol. 72, No. 9
0019-9567/04/$08.00+0 DOI: 10.1128/IAI.72.9.4985–4995.2004


# Cryptococcal Yeast Cells Invade the Central Nervous System via Transcellular Penetration of the Blood-Brain Barrier

Yun C. Chang,[1]† Monique F. Stins,[2]† Michael J. McCaffery,[3] Georgina F. Miller,[4] Dan R. Pare,[5] Tapen Dam,[2] Maneesh Paul-Satyasee,[2] Kwang Sik Kim,[2] and Kyung J. Kwon-Chung[1]*

*Molecular Microbiology Section, Laboratory of Clinical Infectious Diseases,[1] and Comparative Medicine Branch,[5] National Institute of Allergy and Infectious Diseases, and Division of Veterinary Resources,[4] National Institutes of Health, Bethesda, Maryland, and Division of Pediatric Infectious Diseases, Johns Hopkins University School of Medicine,[2] and Department of Biology, Johns Hopkins University,[3] Baltimore, Maryland*

Received 16 April 2004/Returned for modification 20 May 2004/Accepted 2 June 2004

**Cryptococcal meningoencephalitis develops as a result of hematogenous dissemination of inhaled *Cryptococcus neoformans* from the lung to the brain. The mechanism(s) by which *C. neoformans* crosses the blood-brain barrier (BBB) is a key unresolved issue in cryptococcosis. We used both an in vivo mouse model and an in vitro model of the human BBB to investigate the cryptococcal association with and traversal of the BBB. Exposure of human brain microvascular endothelial cells (HBMEC) to *C. neoformans* triggered the formation of microvillus-like membrane protrusions within 15 to 30 min. Yeast cells of *C. neoformans* adhered to and were internalized by the HBMEC, and they crossed the HBMEC monolayers via a transcellular pathway without affecting the monolayer integrity. The histopathology of mouse brains obtained after intravenous injection of *C. neoformans* showed that the yeast cells either were associated with endothelial cells or escaped from the brain capillary vessels into the neuropil by 3 h. *C. neoformans* was found in the brain parenchyma away from the vessels by 22 h. Association of *C. neoformans* with the choroid plexus, however, was not detected during up to 10 days of observation. Our findings indicate that *C. neoformans* cells invade the central nervous system by transcellular crossing of the endothelium of the BBB.**

*Cryptococcus neoformans* causes life-threatening infections primarily in immunocompromised hosts, especially those with impaired cell-mediated immunity, such as patients with human immunodeficiency virus (HIV) infections (25). Although *C. neoformans* can infect any organ, infection of the central nervous system (CNS) is among the most common clinical manifestations, as well as the cause of death. Where HIV is epidemic, *C. neoformans* is the most frequent cause of culture-positive meningoencephalitis (2, 12, 18), which is universally fatal unless it is treated. Even with the most effective fungal therapy, the fatality rate is close to 25%. In HIV patients, life-long maintenance therapy is required with limited options of antimycotic agents (25).

Cryptococcosis originates by inhalation of aerosolized fungal cells, and there is hematogenous spread from the lung to the brain and other organs. In order to cause meningoencephalitis, the fungal cells must survive in the bloodstream and traverse the blood-brain barrier (BBB). The functional sites of the BBB include both the endothelial BBB in the brain microvessels and the epithelial blood-cerebrospinal fluid barrier in the choroid plexus (38). Unlike endothelial cells from peripheral tissues, brain microvascular endothelial cells lack pinocytotic vesicles and are joined by tight junctions (32). These features protect the brain from an unrestricted exchange of molecules between the vascular compartments and the brain (38).

When hematogenously spreading pathogens gain access to the CNS, the major site of entry appears to be the brain microvascular endothelium (24). Although the mechanisms of entry into the CNS for the majority of meningoencephalitis-causing microorganisms are not clear, three potential mechanisms have been described. Pathogens may cross the BBB transcellularly, paracellularly, and/or by means of infected immune cells (Trojan horse mechanism). Transcellular traversal involves penetration of pathogens through the brain microvascular endothelial cells (BMEC). This mode of invasion has been observed for many bacterial pathogens, such as *Escherichia coli* (19, 23, 34), group B *Streptococcus* (31), *Streptococcus pneumoniae* (37), *Listeria monocytogenes* (17), *Citrobacter freundii* (1), *Neisseria meningitidis* (36), and the fungal pathogen *Candida albicans* (22). Paracellular penetration of the BBB has been suggested for the protozoan *Trypanosoma* sp. (16, 27). In the Trojan horse mechanism, infected immune cells, such as monocytes, carry the pathogen through the BBB; this mechanism has been suggested for viral pathogens, such as HIV and simian immunodeficiency virus (13, 15, 26).

*C. neoformans* is thought to invade the brain and cerebrospinal fluid via circulating blood in most clinical situations. In order to penetrate into the brain, *C. neoformans* must cross the endothelium of the BBB or the epithelium of the blood-cerebrospinal fluid barrier. However, the mechanism by which this occurs is one of the least understood steps in CNS cryptococcosis. In a mouse model of meningoencephalitis, Chretien et al. observed *C. neoformans* phagocytosed by host cells that were morphologically consistent with endothelial cells of the leptomeninges (10). This observation was made in mice af-

* Corresponding author. Mailing address: Molecular Microbiology Section, LCI, NIAID Bldg. 10, 11C304, National Institutes of Health, Bethesda, MD 20892. Phone: (301) 496-1602. Fax: (301) 480-3240. E-mail: june_kwon-chung@nih.gov.

† Y.C.C and M.F.S. contributed equally to this work.

flicted with severe leptomeningitis that developed after intravenous injections of *C. neoformans* cells and suggested that *C. neoformans* cells enter the brain by crossing the endothelial BBB. In addition, cryptococci were found to be internalized either by mononuclear cells circulating within meningeal capillaries or by unidentified host cells touching the outer membrane of the capillaries within the meninges. Based on these observations, Chretien et al. hypothesized that *C. neoformans* co-opts monocytes and endothelial cells in order to cross the BBB. The mechanism and sites of the initial cryptococcal entrance into the brain, however, have not been determined. Chen et al. exposed human BMEC (HBMEC) in vitro to *C. neoformans* and assessed the efficiency of yeast cell binding to and traversal across an HBMEC monolayer (9). Although these authors found clear evidence of cryptococcal cells that bound to and crossed the HBMEC monolayer, electron microscopy of numerous samples obtained at different times failed to reveal any *C. neoformans* cells invading the endothelial cells. Since in this study Chen et al. failed to observe *C. neoformans* cells internalized by HBMEC, it was considered unlikely that *C. neoformans* cells traverse the BBB by a transcellular route (9).

In this study we sought to address directly how yeast cells of *C. neoformans* interact with and traverse the BBB by using HBMEC monolayers as an in vitro model of the BBB. We also used an in vivo model of CNS infection involving intravenous injection of *C. neoformans* into mice and monitored the entrance of the yeast cells into the brain. This paper presents the first morphological evidence that *C. neoformans* enters the brain through the endothelial cells of the BBB by a transcellular mechanism.

## MATERIALS AND METHODS

***C. neoformans* strains and media.** Strains of *C. neoformans* serotype D, including strains B-3501, B-4476FO5, and TYCC33, were used in this study. B-3501 and B-4476FO5 are genetically related encapsulated strains, while TYCC33 is an acapsular strain (Δ*cap59*) that is isogenic to B-4476FO5 (5). All strains were maintained on YEPD (1% yeast extract, 2% peptone, 2% glucose) agar slants and stored at 4°C until use. For each experiment, yeast cells were grown on YEPD slants at 30°C for less than 24 h.

**In vitro model of the human BBB with HBMEC.** The source of the BMEC was cerebral cortex specimens obtained from individuals who had undergone surgical resections for treatment of seizure disorders, and the portions with no pathology were used for isolation of BMEC. HBMEC were isolated, characterized, and purified as previously described (40–42). Briefly, HBMEC were purified (>99%) either by isolating small clones of endothelial cells with cloning cylinders or by fluorescence-activated cell sorting by using fluorescently labeled 1,1′-dioctadecyl-1-3,3,3′,3′-tetramethyl-indocarbocyanineperchlorate-labeled acetylated low-density lipoproteins (DiI-AcLDL). In vitro models of the human BBB were constructed by seeding HBMEC on Transwell tissue culture inserts (pore size, 8 or 12 μm; Corning Costar Corp., Cambridge, Mass.) and growing the cells to confluence. This model allowed separate access to the upper compartment (blood side) and the lower compartment (brain side), which allowed mimicking penetration of *C. neoformans* from the vascular system into the brain. The integrity of the BBB models was assessed by measuring the transendothelial electrical resistance (TEER) with a Millicell-ERS apparatus (World Precision Instruments, Sarasota, Fla.) (22, 31). In addition, permeability to small molecules, such as [$^3$H]inulin (molecular weight, 4,000), was assessed as previously described (35, 40).

**Association of *Cryptococcus* with HBMEC.** To investigate the association of *C. neoformans* with HBMEC, HBMEC were seeded in a 24-well plate with RPMI growth medium (41) and grown to confluence in 4 days at 37°C under 5% $CO_2$. Cells of *C. neoformans* grown overnight on a YEPD agar slant were suspended in experimental medium composed of M199 and HAMS-F12 (1:1), counted with a hemocytometer, and added to the HBMEC in experimental medium with 5% human serum. The number of CFU on YEPD agar was used to determine the number of viable cells in the inoculum ($1 \times 10^7$ cells/well). Although a centrifugation step was not necessary for association, as has been shown previously (9), the plates were centrifuged for 5 min at $100 \times g$ to promote contact of *C. neoformans* with HBMEC and were incubated at 37°C for the times indicated below. We did not observe any morphological changes with and without the centrifugation step (data not shown). At each time point during incubation, the HBMEC monolayers were washed four times in experimental medium to remove unattached yeast cells. Subsequently, the HBMEC were lysed with MilliQ water for 30 min, and serial dilutions were made and plated on YEPD agar plates. After 3 days of incubation at 30°C, colonies were counted, and the percentage of the yeast cells associated with the HBMEC was calculated on the basis of the number of CFU in the inoculum.

**Transcytosis of *C. neoformans* in the in vitro model of the human BBB.** To determine the ability of *C. neoformans* yeast cells to cross our in vitro model of the human BBB, *C. neoformans* B-3501, TYCC33, and B-4476FO5 cells ($1 \times 10^5$ cells/well [diameter, 12 mm]) were added to the upper compartment (blood side) of the in vitro BBB model (pore size, 12 μm; constructed as indicated above) and allowed to transmigrate to the lower compartment (brain side). At different times, 100-μl samples were obtained from the bottom compartment (an equal volume of medium was immediately added to maintain a total volume of 1 ml in the bottom compartment) and plated on YEPD agar for determination of the number of CFU. Concurrently, monolayer integrity was assessed by TEER and by measuring permeability of [$^3$H]inulin at the end of the experiment.

**Effect of *C. neoformans* on barrier function of HBMEC measured in real time: ECIS.** To monitor the barrier function of HBMEC exposed to *C. neoformans* in real time, HBMEC were seeded on collagen-coated, gold-plated electrodes in eight-well chamber slides. The slides were connected to an electric cell substrate impedence sensing (ECIS) apparatus (Applied BioPhysics, Troy, N.Y.) that allowed on-line measurements every 2 min, thereby revealing changes in barrier function in real time. After maximal steady-state readings of TEER (~1,500 to 1,800 Ω) were reached, which were indicative of maximal confluence and barrier function, yeast cells of strain B-3501 ($4 \times 10^5$ or $4 \times 10^6$ cells) were added to the ECIS chamber, and changes in the resistance of HBMEC monolayers induced by *C. neoformans* were monitored. Data are expressed below as changes in resistance normalized to time zero values (before exposure to *C. neoformans*) and corrected for control resistance (HBMEC with no exposure to *C. neoformans*).

**Visualization of the interaction of *C. neoformans* with HBMEC in vitro by TEM and by SEM.** To visualize the interaction of *C. neoformans* with HBMEC at the ultrastructural level, HBMEC were seeded on collagen-coated glass coverslips, grown to confluence as described above, and exposed to yeast cells of the encapsulated *C. neoformans* strain B-3501, as well as an acapsular strain (TYCC33). At different times, the monolayers were washed with culture medium and prepared for transmission electron microscopy (TEM) by using a modified method of McCaffery et al. (28). Briefly, HBMEC were fixed with ice-cold 100 mM cacodylate buffer containing 3% formaldehyde, 1.5% glutaraldehyde, and 5 mM $CaCl_2$ (pH 7.4). The HBMEC monolayer and collagen film were peeled off as a whole, rolled up, postfixed in Palade's $OsO_4$ for 1 h at 4°C, stained en bloc in Kellenberger's uranyl acetate, dehydrated through a graded alcohol series, and embedded in Spurr resin. Ultrathin sections were cut with a Leica UCT ultramicrotome, collected on 400-mesh thin bar grids, and poststained in uranyl acetate and lead citrate. The sections were viewed with a Philips EM 420 transmission electron microscope. Images were recorded by using a Soft Imaging system, a Megaview III digital camera, and the analySIS software.

For scanning electron microscopy (SEM), endothelial cells were grown as described above for TEM and exposed to strain B-3501 yeast cells, but they were fixed in 2% glutalaldehyde–2% paraformaldehyde in 0.1 M HEPES buffer containing 3 mM $CaCl_2$ (pH 7.3) at 4°C for 30 min. The HBMEC monolayer was then rinsed in buffer (0.1 M HEPES, 3 mM $CaCl_2$; pH 7.3) three times (10 min each time) at 4°C and postfixed in 1% $OsO_4$–0.8% $KFeCN_6$ in 0.1 M HEPES–3 mM $CaCl_2$ at pH 7.3 for 1 h on ice. After the HBMEC were rinsed in water for 5 min twice, they were stained en bloc with 2% uranyl acetate in water for 2 h in the dark. The HBMEC were dehydrated three times (10 min each time) in a graded ethanol series (up to a final concentration of 100%). Samples were then infused with hexamethyldislazane (Polysciences, Niles, Ill.) for 10 min and allowed to air dry on Whatman no. 1 filter paper. Samples were fixed onto SEM stubs and evaporated with 5-nm chromium by using a Denton DV-502A high-vacuum evaporator operating at 50 mA and $2 \times 10^{-7}$ torr. Samples were viewed and digitized with a Leo 1530 FESEM SEM operating at 1 kV. The images were assembled by using Adobe Photoshop.

**Animal study.** Female BALB/C mice received $10^6$ cells of *C. neoformans* via the tail vein and were examined as follows.

**(i) Determination of the number of CFU from circulating blood and organs.**

In order to determine the number of CFU from circulating blood, animals were bled 0, 0.5, 2, 6, and 24 h after injection. The animals were anesthetized with 3% halothane in a rodent induction chamber and injected with *C. neoformans*. As soon as the injection was complete, the animals were bled from the retroorbital space while they were still under anesthesia (time zero). At the subsequent time points, retroorbital bleeding was performed by using 3% isoflurane as an inhalant anesthetic. Animals were euthanized, the brains and lungs were homogenized, and the homogenates were diluted in phosphate-buffered saline (PBS) and plated on YEPD agar. Blood was diluted fivefold in 0.1% sodium dodecyl sulfate and mixed thoroughly before further dilution in PBS and plating. Colonies were counted after 2 days of incubation at 30°C, and the data are the average counts for three mice at each time point, expressed as percentages of the time zero value. A statistical analysis was performed by using the Student *t* test.

**(ii) Determination of the fungal loads in different parts of the brain.** In order to determine the initial distribution of *C. neoformans* in the brain, the numbers of CFU in different parts of the brain were determined after perfusion. Mice were injected with wild-type strain B-3501 and perfused 3 h after injection. Briefly, mice were anesthetized with pentobarbital sodium (Nembutal Sodium solution; 50 mg/ml; Abbott Laboratories, Chicago, Ill.) that was diluted 1:5 with saline and injected into the peritoneal cavity at a level of approximately 2 mg/mouse. When a mouse achieved a surgical plane of anesthesia, the thoracic cavity was opened, the heart was stabilized with forceps, and the apex was removed with scissors. A blunt 16-gauge needle was introduced into the left ventricle and secured with hemostat forceps. The right atrium was cut, and the mouse was perfused with sterile buffered saline until the perfused saline became colorless. The brain was removed, placed on a sterile acrylic brain matrix (Braintree Scientific, Braintree, Mass.), and sliced into four coronal sections of equal thickness with a sterile blade. Each section of the brain was homogenized and plated on YEPD agar after appropriate dilution in PBS. Colonies were counted after 2 days of incubation at 30°C.

**(iii) Light microscopic visualization of interactions of *C. neoformans* with the brain endothelium. (a) Cryosections.** Infected mice were perfused with 4% formaldehyde in PBS at different times as described above. The brains were removed, sliced into four coronal sections of equal thickness, and soaked in 4% formaldehyde in PBS for 1 h and then in 20% sucrose in PBS overnight. After washing with PBS, the tissue was immersed in OCT Compound 4583 (Sakura Finetek, Torrance, Calif.) in a plastic mold and frozen in 2-methylbutane and dry ice. Cryosectioning (thickness, 15 μm) was performed by Histoserv Inc. (Germantown, Md.), and sections were mounted on microscope slides. The slides were blocked with 2% normal goat serum–1% bovine serum albumin–0.2% Triton X-100 in PBS and incubated with mixture of rabbit anti-factor VIII-Rag antibody (Dako, Carpinteria, Calif.) to visualize the endothelial cell layer of the brain capillaries (21) and with mouse anti-GXM antibody 18B7 (a gift from A. Cassadevall), a cryptococcal polysaccharide capsule-specific antibody, to visualize the yeast cells. After washing, the slides were incubated with the secondary antibodies Alexa Fluor 568 anti-rabbit immunoglobulin G and Alexa Fluor 488 goat anti-mouse immunoglobulin G (Molecular Probes, Eugene, Oreg.). Microscopic imaging was performed with a Zeiss Axioplan and an AxioCam camera (Carl Zeiss, Thornwood, N.Y.) by using the Openlab software imaging system (Improvison, Lexington, Mass.).

**(b) Histopathological sections.** Mice were first perfused with PBS and then with Trump fixative (Electron Microscopy Sciences, Fort Washington, Pa.) at different times after intravenous injection of *C. neoformans* as described above. The brains were removed, embedded in glycol methacrylate, and sectioned before they were stained with toluidine blue at American Histolab, Inc. (Gaithersburg, Md.). The stained sections were examined by light microscopy.

## RESULTS

**Association of *C. neoformans* with HBMEC monolayer.** To determine the association of *C. neoformans* with HBMEC, three strains, B-3501, B-4476FO5, and TYCC33 (Δ*cap59*), were used. Figure 1A shows the time-dependent association of the three *C. neoformans* strains with HBMEC. During the first 45 min, less than 1.5% of the cells of all three strains were found to be associated with HBMEC. At 90 min, TYCC33 cells were two times more efficiently associated with HBMEC than the encapsulated isogenic strain B-4476FO5 cells (9 versus 4.3%), while the highly encapsulated strain, B-3501, was the strain that was least able (1.5 to 2.0%) to associate with HBMEC. At 3 h, the number of cells associated with the HBMEC was similar to the number observed at 90 min. By 6 h, the differences in association with HBMEC between B-4476FO5 and TYCC33 became insignificant. These differences were not the result of decreased viabilities of the three *C. neoformans* strains since we observed no change in viability when organisms were incubated in experimental medium with serum for up to 24 h (data not shown). Exposure of HBMEC to all three cryptococcal strains did not affect HBMEC viability as determined with a live/dead stain (Molecular Probes), with which the cytoplasm of live cells was stained with fluorescent calceinAM while the nuclei of dead cells were stained with ethidium heterodimer (data not shown). These findings suggest that the association of the acapsular strain, TYCC33, with HBMEC appeared to be saturated at 90 min, whereas the association of the encapsulated strains, B-4476FO5 and B-3501, increased with time for up to 6 h of incubation. *C. neoformans* association with HBMEC, therefore, appears to be influenced by the presence of the capsule.

**Transcytosis of *C. neoformans* in the in vitro model of BBB.** The time course of *C. neoformans* traversal was determined by using our in vitro human BBB model system. Although all three yeast strains added to the upper chamber (blood side) of the BBB models transmigrated to the bottom chamber (brain side) by 3 h, the acapsular strain (TYCC33) yielded the lowest number of CFU at all times (Fig. 1B). The number of CFU that traversed the HBMEC increased steadily for the thin-capsule strain (B-4476FO5), whereas the number of CFU of the thick-capsule strain (B-3501) remained the same after 9 h of incubation. This finding indicated that although the encapsulated cells associated less efficiently with the HBMEC than the acapsular cells (TYCC33), they traversed the HBMEC more efficiently than the acapsular cells. The degree of capsule thickness did not appear to affect the traversal of yeast cell across the HBMEC significantly. We next examined the effect of *C. neoformans* traversal on HBMEC monolayer integrity, as measured by TEER and inulin permeability at the end of the transcytosis experiment. The TEER values remained similar for HBMEC without *C. neoformans* ($150 \pm 15\ \Omega/cm^2$) and HBMEC exposed to B-3501 ($165 \pm \Omega/cm^2$) during the 12-h transcytosis experiment. The inulin permeabilities of HBMEC monolayers before B-3501 cells crossed ($2.5\% \pm 0.1\%$) and after B-3501 cells crossed ($2.2\% \pm 0.1\%$) also were not significantly different. These findings indicate that *C. neoformans* yeast cells crossed the HBMEC monolayers without any change in the integrity of the HBMEC. The barrier integrity of HBMEC during exposure to cryptococcal yeast cells was also assessed by ECIS. As shown in Fig. 1C, when an inoculum of $4 \times 10^5$ yeast cells/well was used, the HBMEC monolayer barrier remained unchanged until at least 20 h after inoculation. In contrast, when an inoculum of $4 \times 10^6$ cells/well was used, the ECIS data indicated that the HBMEC barrier function was maintained only for up to 15 h. These data indicated that the integrity of the HBMEC barrier was dependent on the number of yeast cells added to the well but was maintained for up to 15 h of incubation with cryptococci. Since we assessed transcytosis for up to 12 h with an inoculum of $1 \times 10^5$ cells/well, the yeast cells obtained from the bottom chamber most likely represented the cells that migrated across an intact HBMEC monolayer.

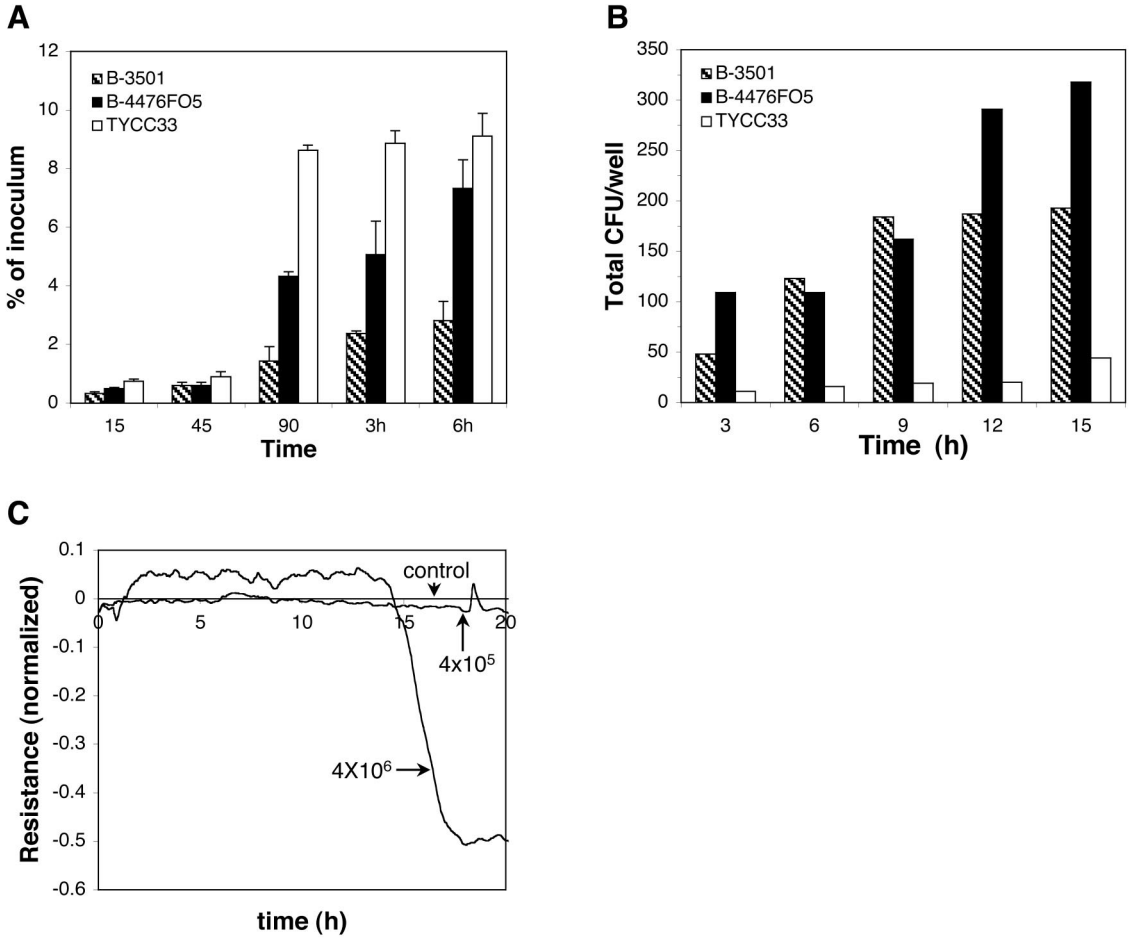


FIG. 1. Association with and traversal of HBMEC by *C. neoformans*. (A) Association of strains B-3501 (encapsulated), B-4476FO5 (encapsulated), and TYCC-33 (Δ*cap59*, acapsular) assessed at different times. The error bars indicate standard deviations. (B) Transcytosis of *C. neoformans* across HBMEC monolayers. HBMEC monolayers were exposed to B-3501, B-4476FO5, or TYCC33 ($1 \times 10^5$ cells/well), and the numbers of CFU transcytosed across the HBMEC at different times were determined. The values are the averages for two different samples of each strain at each time. The experiment was repeated, and similar results were obtained. (C) Effect of *C. neoformans* cells on the barrier function of HBMEC as measured by an ECIS apparatus after addition of B-3501 ($4 \times 10^6$ or $4 \times 10^5$ cells/well) to an HBMEC monolayer.

**Ultrastructural visualization of the interaction between *C. neoformans* and HBMEC.** The interaction between *C. neoformans* cells and HBMEC was studied at the ultrastructural level. SEM allows observation of large surface areas with relatively rare adherence events, but the process of internalization can be more readily documented with TEM. Therefore, we used SEM to study the interaction of yeast cells with the HBMEC surface and TEM for examination of intracellular organelles involved in the adherence of *C. neoformans* and its entry into the HBMEC.

**(i) SEM.** Control HBMEC monolayers not exposed to yeast cells had a smooth surface without membrane protrusions (Fig. 2A). In contrast, as early as 15 min after exposure to strain B-3501 yeast cells, microvillus formation on the surface of HBMEC became evident (Fig. 2B), and by 30 min numerous microvilli had surrounded the yeast cells attached to the HBMEC surface (Fig. 2C). Yeast cells starting to penetrate the HBMEC were observed after 30 min (Fig. 2D), and yeast cells partially engulfed by the HBMEC membrane were evident at this time (Fig. 2E). No yeast cells were found in association with areas between two adjacent HBMEC or close to junctions.

**(ii) TEM.** Since the extracellular capsule is a major virulence factor of *C. neoformans* and an acapsular strain has been shown to be avirulent (5), we used an encapsulated strain (B-3501) and an acapsular mutant (TYCC33) for the TEM studies. The morphological features of HBMEC interacting with encapsulated and acapsular yeast cells were similar. Figure 3 illustrates the sequential events that led to engulfment of B-3501 cells and TYCC33 cells by HBMEC. Upon exposure to yeast cells, HBMEC produced numerous microvillus-like membrane protrusions within 15 to 30 min regardless of the presence of capsule. A considerable number of membrane protrusions were seen in HBMEC within 30 min upon exposure of the monolayer to B-3501 cells (Fig. 3A), while no such changes were seen in uninfected control HBMEC (data not shown). Within 2 h of exposure, there were numerous acapsular cells that were entering the HBMEC or lodged in the cytoplasm of the HBMEC, while internalized encapsulated yeast cells were found at 6 h. Figure 3B shows numerous microvillus-like protrusions of HBMEC embracing the daughter cell of an acapsular yeast at 2 h, suggesting that there was partial engulfment. Some strands of the microvilli adhered to

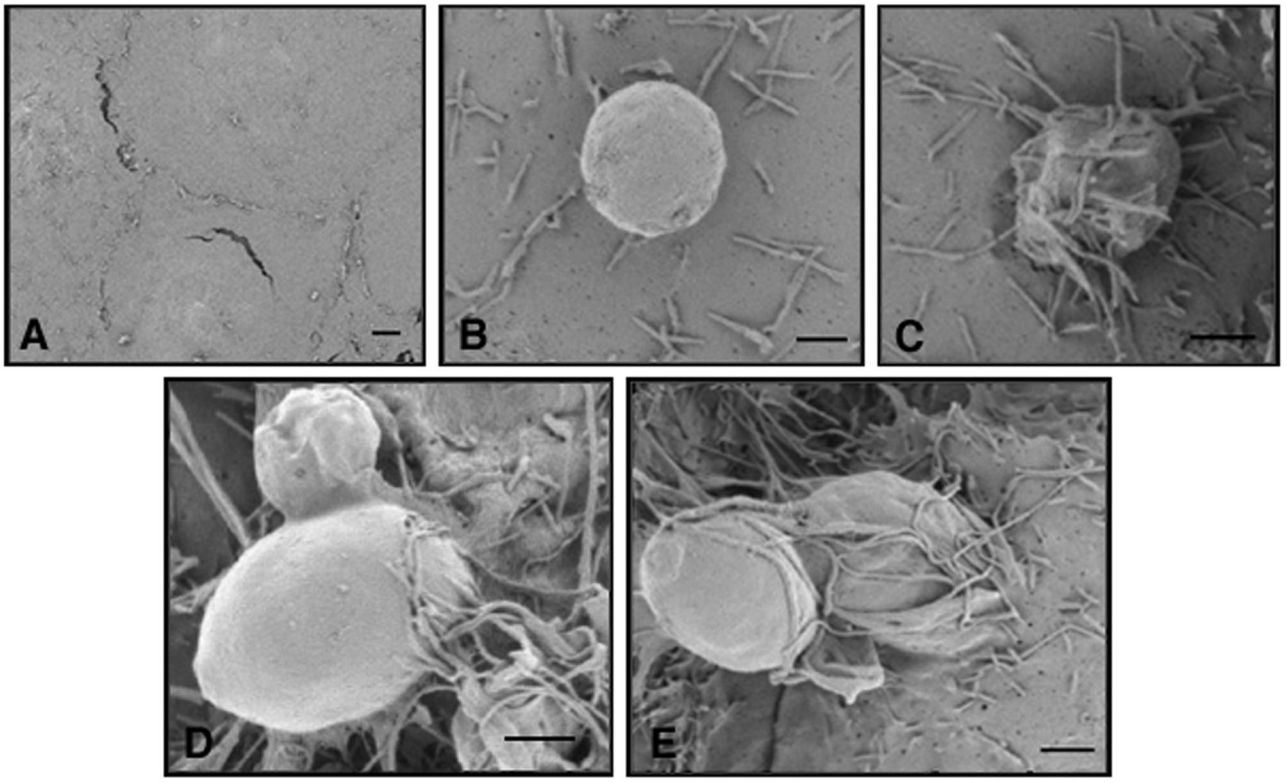


FIG. 2. SEM results. (A) Surface of the HBMEC at time zero (control). (B) Extensive microvillus-like projections observed 15 min after addition of B-3501 cells to an HBMEC monolayer. (C) Microvillus-like projections covering yeast cells at 30 min. (D and E) Penetration of yeast cells into HBMEC. Scale bars = 4 μm.

the wall of the mother cell. Figure 3C shows an internalized encapsulated mother cell with a daughter cell still remaining outside the BMEC (after 6 h of incubation). Figures 3D and E show completely internalized *C. neoformans* cells within the cytoplasm proximal to the nuclei of HBMEC. In spite of their large size, both encapsulated yeast cells (Fig. 3D) and acapsular yeast cells (data not shown) were present within a vacuole. Some yeast cells were seen at the basolateral side of the monolayer after 6 h (Fig. 3F), suggesting that there was complete crossing of HBMEC by this time. At each time, no yeast cells were associated with the junctions of HBMEC, and none were found between adjacent HBMEC. The HBMEC containing *C. neoformans* cells had no ultrastructural changes; the morphology of the nucleus, mitochondria, and endoplasmic reticulum of exposed HBMEC was unchanged when these cells were compared to the control monolayer that was not exposed to *C. neoformans* (data not shown). We found no indication that cellular damage, apoptosis, or disruption of tight junctions occurred at the times studied. Together with the transcytosis data, these findings indicated that yeast cells of *C. neoformans* penetrated the HBMEC transcellularly regardless of the capsule phenotype without causing any change in the integrity of the HBMEC or injury to the HBMEC monolayer.

***C. neoformans* in circulating blood, lungs, and brain after intravenous injection.** Since *C. neoformans* hematogenously invades the brain tissue by crossing the BBB, we studied the kinetics of *C. neoformans* in circulating blood at different times after intravenous injection of an isogenic set of encapsulated (B-4476FOA) and acapsular (TYCC33) strains. Dramatic decreases in the number of CFU of both encapsulated and acapsular strains were seen in circulating blood: only 1.7 to 2.0% of the time zero numbers of CFU were found in the bloodstream after 30 min (Fig. 4). These dramatic reductions in the number of CFU in the circulating blood after 30 min indicate that the host defense system efficiently cleared the organisms from the bloodstream. The number of CFU of the encapsulated strain decreased further to less than 0.2% in 24 h (Fig. 4A), while the acapsular strain nearly disappeared from the blood by 2 h (Fig. 4B). Significant decreases in the number of CFU were also observed in the lungs and the brain by 30 min postinjection. Since the mice were not perfused, the CFU in the brain and the lungs at time zero mostly represented the yeast cells circulating in the vascular systems of the two organs. There was no significant difference ($P > 0.10$) in the numbers of CFU found in the brain between 30 min and 24 h postinjection in mice that received either encapsulated cells or acapsular cells. However, the number of CFU in the lungs decreased considerably between 30 min and 24 h for both the acapsular ($P = 0.03$) and encapsulated ($P = 0.017$) strains. The percentage of CFU was lower in the lungs than in the brain for both encapsulated and acapsular strains by 24 h. This may have been due to the greater fungicidal capacity of alveolar macrophages compared with that of the brain cells. Since most of the yeast cells were cleared from the bloodstream after 0.5 h, the CFU found in the brain and the lungs between 0.5 and 24 h likely represented the cells that had already adhered to the endothelium and/or had

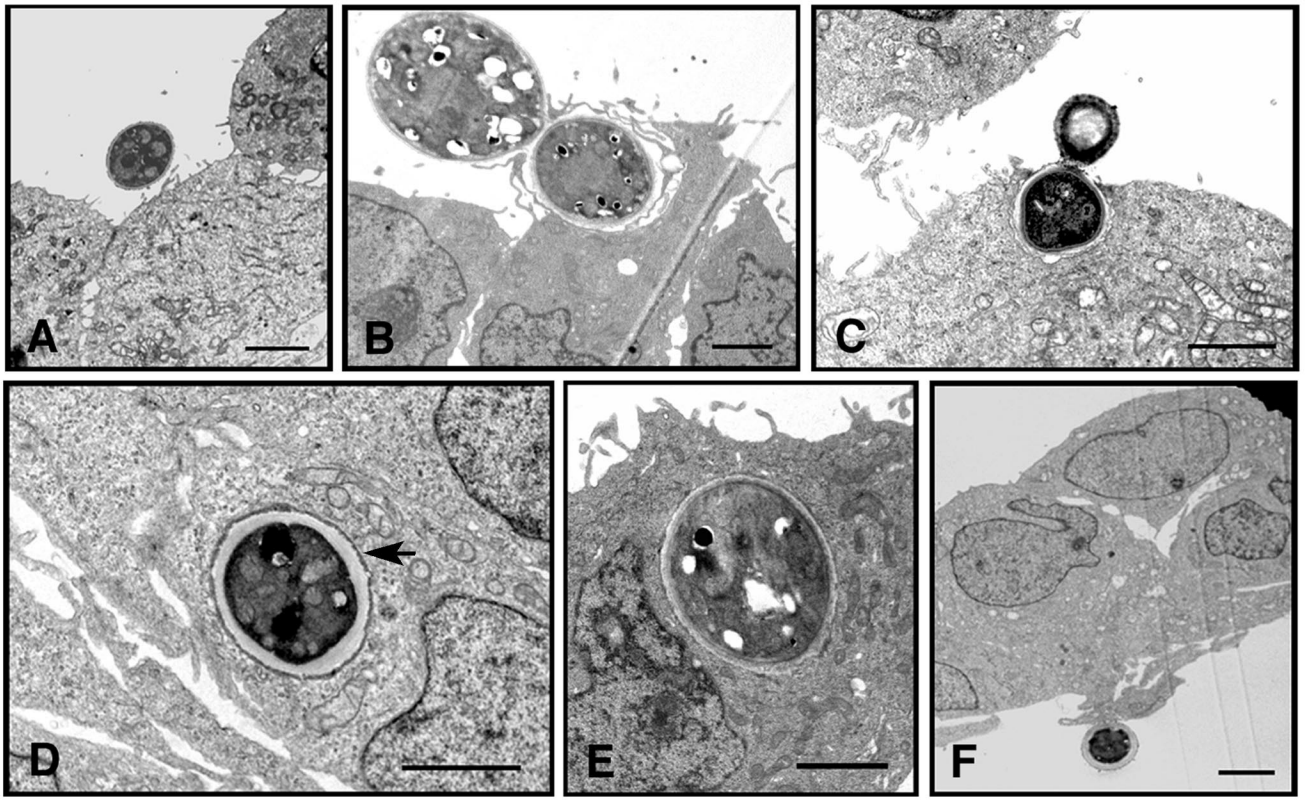


FIG. 3. TEM results. (A) Formation of microvillus-like projection by HBMEC upon exposure to B-3501 cells. (B) TYCC33 yeast cell partially engulfed by HBMEC at 2 h. (C) Partially internalized budded cells of B-3501 at 6 h. (D and E) Cell of B-3501 completely internalized in the cytoplasm proximal to nuclei of HBMEC. The arrow in panel D indicates a vacuole. (F) Cell of B-3501 attached to the basolateral side of HBMEC after the HBMEC layer was crossed. Scale bars = 4 μm.

become established in the tissue. It is not clear whether the distribution of *C. neoformans* is random throughout the brain or whether *C. neoformans* is associated preferentially with certain areas of the brain during the early stages of infection. Therefore, the fungal loads in different parts of the brain were determined at 3 and 24 h by using three mice perfused at each time. The numbers of CFU found in the cerebellum and in the middle and front parts of the brain were not significantly different (data not shown). In addition, as determined by microscopic examination of the cryosections, we found no preferen-

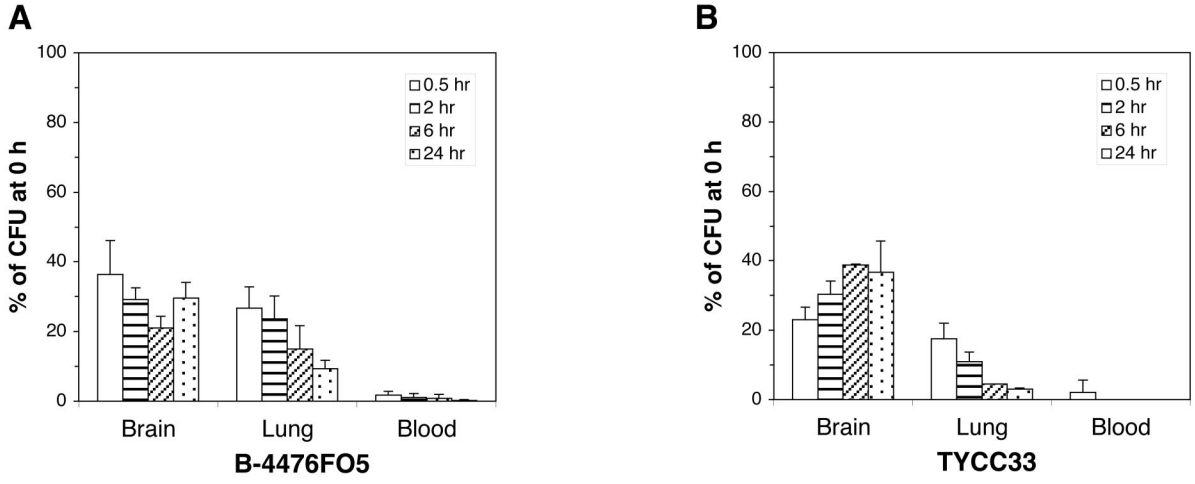


FIG. 4. CFU recovered from the brain, lungs, and blood of mice ($n$ = 3 for each time) injected with encapsulated cells (B-4476FO5) and isogenic acapsular cells (TYCC33). The CFU values are expressed as percentages of the counts at time zero. At time zero, the CFU from the brain and the lungs represent the CFU in the bloodstream circulating in the two organs. The error bars indicate standard deviations.

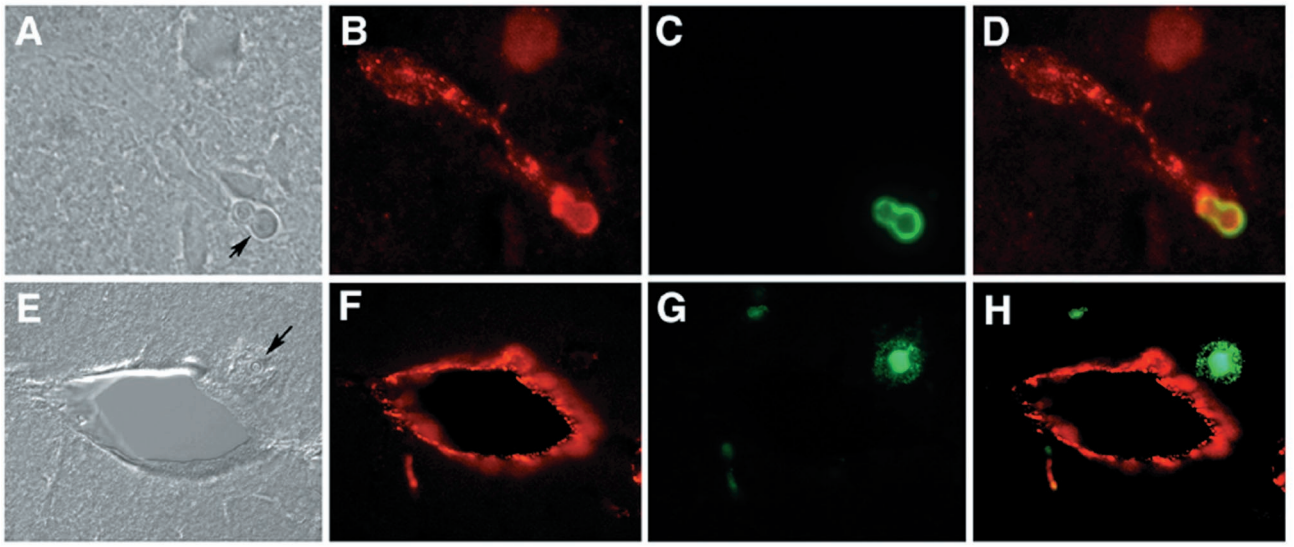


FIG. 5. Immunostaining of cryosections prepared from mouse brain injected with B-3501. The sections were stained with a monoclonal anticapsular antibody (green) and anti-human factor VIII (red). (A) Cryosection prepared at 3 h postinjection (differential interference contrast microscopy). The arrow indicates a yeast cell. (B) Image matching the image in panel A, showing factor VIII-stained endothelium. (C) Field shown in panel B, showing a yeast cell stained with anticapsular antibody. (D) Superimposition of panels B and C, showing the yeast cell directly associated with endothelium. (E) Cryosection prepared at 22 h postinjection (differential interference contrast microscopy). The arrow indicates a yeast cell. (F) Fluorescent micrograph of panel E, showing a cross section of a capillary in the brain parenchyma. (G) Field shown in panel E, showing a yeast cell with a diffuse capsule. (H) Superimposition of panels G and H, showing a yeast cell in brain parenchyma outside the vessel.

tial distribution of *C. neoformans* cells in any particular section of the brain at the early time point (data not shown).

**Light microscopic visualization of frozen sections stained with fluorescent antibody.** To examine the physical relationship between cryptococcal cells and the vascular system, as well as the brain parenchyma, we determined the location of cryptococcal cells in cryosections of the perfused brains at different times after injection. An association of the cryptococcal cells with microvascular endothelium could be clearly determined by immunofluorescence microscopy. Cryptococcal yeast cells localized inside the brain proximal to capillaries were detected as early as 3 h postinoculation, indicating that the yeast was crossing the BBB (Fig. 5A to D) at this early time. At 22 h postinfection, some yeast cells were localized away from the vessels (Fig. 5E to H), indicating that there was migration of yeast cells into the neuropil. Interestingly, at 3 h postinfection the anticapsular antibody detected the presence of GXM in yeast cells as well-defined fluorescence around the cell surface (Fig. 5A and C). However, at 22 h postinfection, GXM fluorescence was also observed as diffused patches around the yeast cells (Fig. 5E and G), suggesting that cryptococcal cells shed the capsule component in the brain parenchyma as infection progressed.

**Histopathology.** To further confirm the immunocytochemical findings for the association of *C. neoformans* cells with the endothelium and to obtain a better understanding of the morphology, thoroughly perfused brain tissues were also imbedded in glycol methacrylate. In toluidine blue-stained sections, the brain tissue was blue, while *C. neoformans* cells stained pink. Very few *C. neoformans* cells were present in the brain at 3 h postinjection. When detected, however, the yeast cells were always closely associated with the brain capillaries and were rarely found within the brain parenchyma (Fig. 6A and B). By 22 h postinjection, yeast cells were readily found in the brain parenchyma near the capillaries (data not shown). At 10 days postinjection, brains showed large cystic lesions throughout the brain parenchyma. Notably, the largest numbers of yeast cells were localized in perivascular cysts (Fig. 6C to E), and some yeast cells were closely associated with cells morphologically consistent with endothelial cells (Fig. 7A and B). A few yeast cells appeared to be in the process of crossing the microvessels into the perivascular area, as shown in Fig. 6D. The choroid plexus and meninges remained free of yeast cells at early times (Fig. 7C and D), and yeast cells were only infrequently observed in the subarachnoid space at 10 days (Fig. 7E). Occasional clusters of yeast cells in the brain parenchyma just beneath the pia matter appeared to be breaking into the subarachnoid space (Fig. 7F). A cystic lesion containing a large number of yeast cells beneath the pia matter was also observed at 10 days (Fig. 7G). The choroid plexus, however, remained free of yeast cells at this time (Fig. 7C).

## DISCUSSION

The BBB is a structural and functional barrier that is formed by BMEC. BMEC possess distinct features, such as tight junctions between the cells and low rates of pinocytosis (32). The BBB protects the brain from any microorganisms and toxins circulating in the blood. Recent studies, however, have shown that meningitis-causing microorganisms can cross the BBB (24). Many bacterial pathogens use a transcellular mechanism to penetrate the BMEC, although some reports have suggested that Ly-6C$^{high}$ monocyte subpopulations transport *L. monocytogenes* into mouse brains by a Trojan horse mechanism (14). A

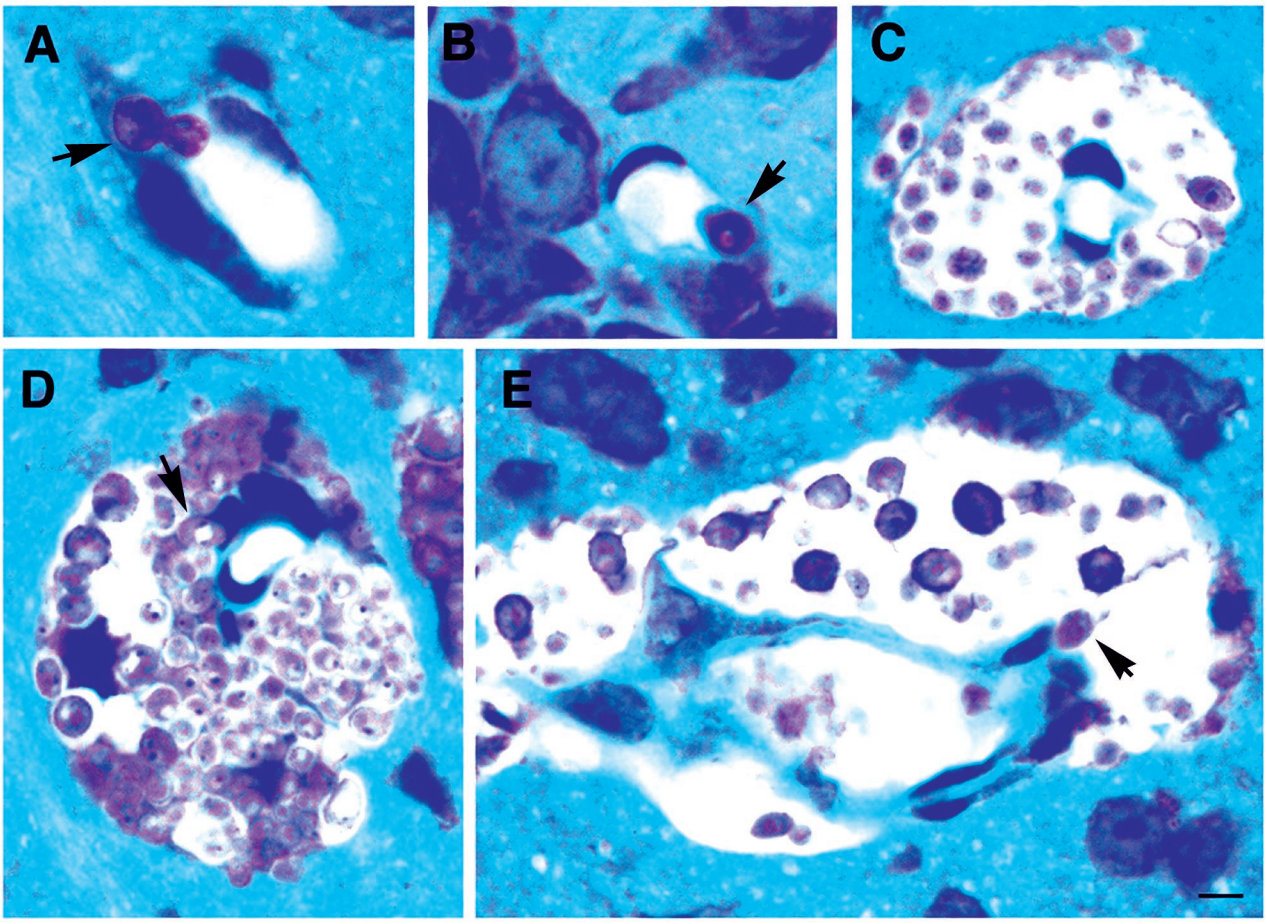


FIG. 6. Histological sections of mouse brain stained with toluidine blue. (A) Yeast cell (arrow) localized at the interface of a vessel and the neuropil at 3 h postinjection. The image suggests that the yeast cell is moving out of the vessel into the brain. (B) *C. neoformans* cell (arrow) closely associated with an endothelial cell (3 h postinjection) of a vessel in the brain parenchyma. (C) Perivascular cystic lesion formed by replication of *C. neoformans* (10 days). (D) Perivascular growth of *C. neoformans* (10 days). Some yeast cells are in the process of transmigrating from endothelial cells to the brain (the arrow indicates a yeast cell which is closely associated with an endothelial cell). (E) Cross section of a microvessel, showing the perivascular concentration of yeast cells and a yeast cell apparently leaving a vessel lumen (arrow). Scale bar = 4 μm.

recent study with a phospholipase-deficient strain of *C. neoformans* showed that mutants could establish a CNS infection if they were presented within monocytes or from a culture derived from cells engulfed by mononuclear phagocytes but not if they were injected directly into the venous circulation (39). The authors concluded that mononuclear phagocytes are a vehicle for cryptococcal dissemination to the brain. This suggests that a Trojan horse mechanism is a possible means of brain invasion by *C. neoformans*. The previous study, however, did not allow distinction between cryptococci which entered the brain directly by crossing the BBB and cryptococci which entered via a Trojan horse mechanism. Furthermore, all cryptococcal yeasts that were in the process of escaping from the endothelial cells into the neuropil during the early time of our study were free of any type of host immune cells. In this study, we showed for the first time that *C. neoformans* adheres to and traverses across HBMEC by a transcellular mechanism.

The in vitro interactions between *C. neoformans* and endothelial cells were studied previously by using human umbilical vein endothelial cells (HUVEC). Ibrahim et al. reported that acapsular *C. neoformans* cells adhered to and were phagocytosed by HUVEC more efficiently than encapsulated cells were. Both acapsular and encapsulated cells caused endothelial cell injury, but the acapsular cells caused greater injury than the encapsulated cells caused. Internalization of *C. neoformans* by HUVEC was blocked by cytochalasin D, suggesting that the internalization occurred by phagocytosis (20). These observations suggest that *C. neoformans* cells escaped from the intravascular compartment by transcellular traversal across the endothelial cell layer. However, it is not clear whether the information derived from HUVEC is relevant to cryptococcal traversal of HBMEC. It has previously been shown that the interactions of meningitis-causing bacteria with endothelial cells are different for HBMEC and HUVEC (34).

Our investigation of cryptococcal interactions with HBMEC revealed that both encapsulated and acapsular yeast cells adhere to and traverse across HBMEC monolayers without affecting the monolayer morphology or integrity. The ECIS, TEER, and [$^3$H]inulin permeability data indicated that the brain endothelial barrier property was maintained for at least 15 h after exposure to encapsulated *C. neoformans* cells ($4 \times 10^6$ cells), and no breach of the barrier occurred during the

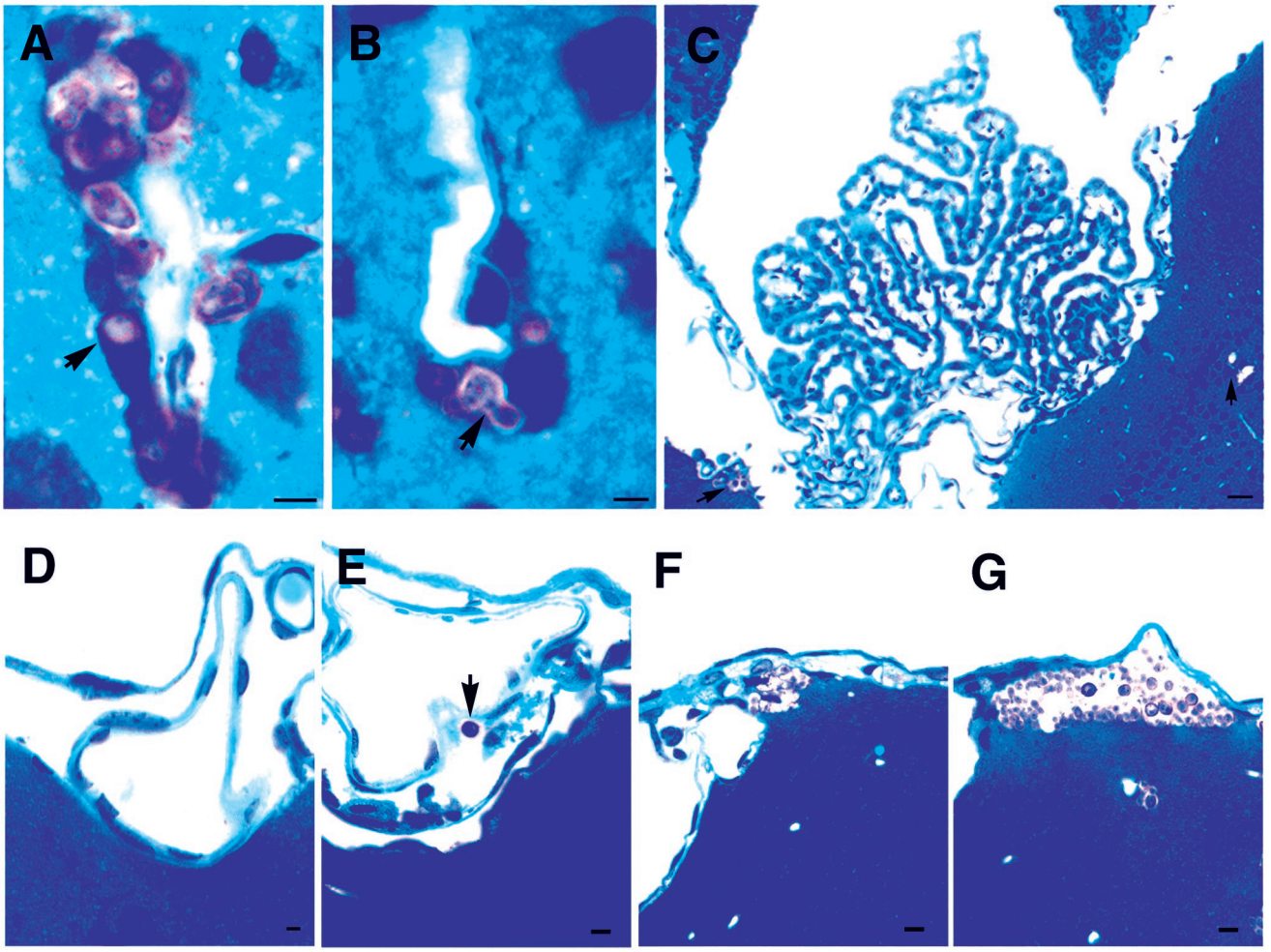


FIG. 7. Histological sections of mouse brain stained with toluidine blue. (A and B) *C. neoformans* cells lodged in endothelial cells of brain microvessels (10 days). (C) Choroid plexus remained normal and free of *C. neoformans* cells at 10 days postinjection, while cryptococcal lesions were seen in the nearby brain parenchyma (arrows). (D) Meninges free of *C. neoformans* 22 h postinjection. (E to G) *C. neoformans* was present in the subarachnoid space (arrow) or just under the pia matter of meninges by 10 days postinjection. Scale bars = 4 μm.

time period studied (up to 24 h) when $4 \times 10^5$ cells or a smaller inoculum was added to HBMEC. Since we found that yeast cells crossed HBMEC before 12 h, the traversal of *C. neoformans* is unlikely to be the result of altered integrity or a leaky HBMEC monolayer. These findings differ from those of Chen et al. (9), who reported morphological changes in the nucleus, mitochondria, and endoplasmic reticulum in HBMEC upon exposure to *C. neoformans* ($10^6$ cells/well), as well as disruption of the HBMEC junctions at 16 h. This discrepancy could have been due to differences in the ages and sizes of the fungal inocula or to reagents, such as the batches of serum used, as well as the status of the HBMEC monolayer. In addition, we used primary HBMEC, while Chen et al. used simian virus 40-transformed HBMEC (9).

Acapsular cells of *C. neoformans* adhered to and invaded the HBMEC monolayer more efficiently than cells of the encapsulated strains, as observed in the TEM preparations. Penetration of the HBMEC by acapsular cells was seen in 2 h, while penetration of the HBMEC by encapsulated cells was not observed until 6 h. Similar observations have been made with HBMEC association assays, in which higher numbers of acapsular cells than of encapsulated cells were found associated with a monolayer. Similar results have been reported for other cell lines, including lung epithelial cells (29), rat glial cells (30), and HUVEC (20). Although we centrifuged the plates to synchronize and promote contact between HBMEC and the cryptococcal cells, encapsulated cells tended to float more readily than acapsular cells, presumably due to their buoyancy. The buoyancy might have caused the encapsulated cells to be less efficient in invasion of the HBMEC prepared for the TEM study. Since SEM allows examination of a large surface area, relatively rare events can be more readily spotted with SEM than with TEM. By using SEM, we detected some encapsulated cells in the process of penetrating the HBMEC after 30 min of incubation.

Although the acapsular cells efficiently adhered to and invaded the HBMEC, the number of CFU that traversed the HBMEC was significantly lower than the numbers of CFU of the encapsulated strains that traversed the HBMEC. It is not

clear if the acapsular cells were killed more efficiently inside the HBMEC or if the HBMEC used different pathways to handle the invading acapsular and encapsulated cells. It is also possible that the rate at which acapsular strain cells got through the endothelial cells was simply low. Interestingly, the fungal burdens in the brains of infected mice were similar for acapsular and capsular strains for up to 24 h for unperfused mice (Fig. 4). Since for the most part both acapsular and encapsulated *C. neoformans* cells were cleared from the circulating blood by 0.5 h postinjection, the CFU obtained from the brain 0.5 h after injection likely represented the cells associated with the endothelium in addition to the cells that were already in the brain tissue. Acapsular strains are known to be avirulent in mice (5–8), and mice infected with acapsular cells contain yeast cells in the brain during early times but are healthy with no fungus in the brain at the time that mice infected with the encapsulated yeast succumb to a fatal cryptococcosis (4). Our in vitro data suggest that acapsular yeasts do not cross the BBB as efficiently as encapsulated cells. This could contribute to the diminished virulence of acapsular yeasts. To examine the efficiency with which acapsular and encapsulated cells cross the BBB in vivo, further assessment of fungal burdens at various times by using perfused mice is necessary. The biological function of the microvascular system in the CNS is regulated by paracrine interactions between parts of a capillary complex that includes the capillary endothelium, the pericytes, the astrocyte foot processes, the smooth muscle cells, and neuronal endings (11, 33). Since the in vitro HBMEC model that we used in this study is composed of endothelial cells and devoid of the other components of the barrier, we used in vivo models to examine the early events of *C. neoformans* entry into the CNS. In the mouse model, the cells of *C. neoformans* were associated with the BBB at 3 h postinjection. The histological sections offered inadequate resolution for determination of the exact position of *C. neoformans* cells. However, yeast cells were closely associated with the endothelial cells or located at the interface of the vessel and neuropil. Thus, our in vitro and in vivo data are in accordance with each other and corroborate the validity of using the in vitro BBB system to characterize the initial events of *C. neoformans* entry into the CNS (i.e., the interaction with HBMEC).

Apparently, brain capillaries, and not the choroid plexus, are important routes for the entrance of circulating *C. neoformans* into the brain, which causes cryptococcal meningoencephalitis. Most of the *C. neoformans* cells observed in the early stages of infection were located around the capillary vessels in brain parenchyma. *C. neoformans* requires aeration for optimum growth. Upon traversal from the capillary BBB, the yeast cells appear to have multiplied initially when the oxygen tension is high. However, based on the numbers of CFU in the four different coronal sections of the brain at 3 h, we found no significant differences in the initial distribution of *C. neoformans* cells. The extensive neural microvascular network probably allows entry of *C. neoformans* yeast cells into the neuropil throughout the brain. By 10 days postinjection, *C. neoformans* cells were widely distributed throughout the brain parenchyma and the meninges, excluding the choroid plexus. This suggests that *C. neoformans* entered the brain by penetration of the endothelial BBB and spread to the meninges. These observations are consistent with human cryptococcal meningoencephalitis, in which ventricultis is usually not present and intrathecal antimycotic therapy is ineffective (J. E. Bennett, National Institutes of Health, personal communication).

At present, the *C. neoformans* components required for interactions with HBMEC have not been identified. Numerous cryptococcal factors have been shown to contribute to the pathogenesis of *C. neoformans*, including the capsule, laccase, phospholipase B, and other factors (3). However, except for the capsule, the roles of these factors in traversal of yeasts across the BBB have not been investigated. Further studies are needed to determine whether virulence factors such as laccase and phospholipases play an important role in the interaction with HBMEC. Future work is also needed to understand the mechanisms that are involved in the HBMEC actin cytoskeletal rearrangements and relevant signaling pathways for *C. neoformans* internalization and traversal of HBMEC.

In conclusion, in this report we present two sets of findings that for the first time indicate that entry of *C. neoformans* cells into the CNS occurs via transcellular crossing of the BMEC. First, in our in vitro study, SEM revealed that yeast cells penetrating HBMEC were associated with microvillus-like protrusions at the entry site on the surface of HBMEC. We also showed by using TEM that *C. neoformans* cells penetrating the HBMEC monolayers were localized in the enclosed vacuole within the HBMEC, and no *C. neoformans* cells were found between HBMEC. Second, our in vivo study showed that there were *C. neoformans* cells within the microvascular endothelial cells in the mouse brain 3 h after intravenous injection of *C. neoformans*, and clusters of *C. neoformans* were present in the brain parenchyma at 22 h postinjection. *C. neoformans* cells lodged in the BMEC were frequently seen in histologic sections within 10 days. Association of *C. neoformans* with the meninges was not observed during the early times but was observed by day 10, while no yeast cells were observed in the choroid plexus. Taken together, our in vitro and in vivo studies suggest that the initial site of cryptococcal entry into the brain is the endothelial BBB and that cryptococcal traversal of HBMEC monolayers occurs via a transcellular mechanism.

## ACKNOWLEDGMENTS

We are grateful to Tiffany Gough and Donna Pearce for experimental assistance and Ashok Varma for reading the manuscript.

This work was supported in part by NIH grant MH63850 to M.F.S. and by NIH grants NS 26310 and A1 47225 to K.S.K.

## REFERENCES

1. **Badger, J. L., M. F. Stins, and K. S. Kim.** 1999. *Citrobacter freundii* invades and replicates in human brain microvascular endothelial cells. Infect. Immun. **67:**4208–4215.
2. **Bogaerts, J., D. Rouvroy, H. Taelman, A. Kagame, M. A. Aziz, D. Swinne, and J. Verhaegen.** 1999. AIDS-associated cryptococcal meningitis in Rwanda (1983–1992): epidemiologic and diagnostic features. J. Infect. **39:**32–37.
3. **Buchanan, K. L., and J. W. Murphy.** 1998. What makes *Cryptococcus neoformans* a pathogen. Emerg. Infect. Dis. **4:**71–83.
4. **Chang, Y. C., R. Cherniak, T. R. Kozel, D. L. Granger, L. C. Morris, L. C. Weinhold, and K. J. Kwon-Chung.** 1997. Structure and biological activities of acapsular *Cryptococcus neoformans* 602 complemented with the *CAP64* gene. Infect. Immun. **65:**1584–1592.
5. **Chang, Y. C., and K. J. Kwon-Chung.** 1994. Complementation of a capsule-deficient mutation of *Cryptococcus neoformans* restores its virulence. Mol. Cell. Biol. **14:**4912–4919.
6. **Chang, Y. C., and K. J. Kwon-Chung.** 1998. Isolation of the third capsule-associated gene, *CAP60*, required for virulence in *Cryptococcus neoformans*. Infect. Immun. **66:**2230–2236.
7. **Chang, Y. C., and K. J. Kwon-Chung.** 1999. Isolation, characterization, and

localization of a capsule-associated gene, *CAP10*, of *Cryptococcus neoformans*. J. Bacteriol. **181:**5636–5643.
8. **Chang, Y. C., L. A. Penoyer, and K. J. Kwon-Chung.** 1996. The second capsule gene of *Cryptococcus neoformans*, *CAP64*, is essential for virulence. Infect. Immun. **64:**1977–1983.
9. **Chen, S. H. M., M. F. Stins, S. H. Huang, Y. H. Chen, K. J. Kwon-Chung, Y. C. Chang, K. S. Kim, K. Suzuki, and A. Y. Jong.** 2003. *Cryptococcus neoformans* induces alterations in cytoskeleton of human brain microvascular endothelial cells. J. Med. Microbiol. **52:**961–970.
10. **Chretien, F., O. Lortholary, I. Kansau, S. Neuville, F. Gray, and F. Dromer.** 2002. Pathogenesis of cerebral *Cryptococcus neoformans* infection after fungemia. J. Infect. Dis. **186:**522–530.
11. **Cohen, Z., M. Ehret, M. Maitre, and E. Hamel.** 1995. Ultrastructural analysis of tryptophan hydroxylase immunoreactive nerve terminals in the rat cerebral cortex and hippocampus: their associations with local blood vessels. Neuroscience **66:**555–569.
12. **Currie, B. P., and A. Casadevall.** 1994. Estimation of the prevalence of cryptococcal infection among patients infected with the human immunodeficiency virus in New York City. Clin. Infect. Dis. **19:**1029–1033.
13. **Dallasta, L. M., L. A. Pisarov, J. E. Esplen, J. V. Werley, A. V. Moses, J. A. Nelson, and C. L. Achim.** 1999. Blood-brain barrier tight junction distribution in human immunodeficiency virus-1 encephalitis. Am. J. Pathol. **155:** 1915–1927.
14. **Drevets, D. A., M. J. Dillon, J. S. Schawang, N. Van Rooijen, J. Ehrchen, C. Sunderkotter, and P. J. Leenen.** 2004. The Ly-6C(high) monocyte subpopulation transports *Listeria monocytogenes* into the brain during systemic infection of mice. J. Immunol. **172:**4418–4424.
15. **Erlander, S. R.** 1995. The solution to the seven mysteries of AIDS: the 'Trojan horse.' Med. Hypotheses **44:**1–9.
16. **Grab, D. J., O. Nikolskaia, Y. V. Kim, J. D. Lonsdale-Eccles, S. Ito, T. Hara, T. Fukuma, E. Nyarko, K. J. Kim, M. Stins, M. J. Delannoy, J. Rodgers, and K. S. Kim.** African trypanosome interactions with an in vitro model of the human blood-brain barrier. J. Parasitol., in press.
17. **Greiffenberg, L., W. Goebel, K. S. Kim, I. Weiglein, A. Bubert, F. Engelbrecht, M. Stins, and M. Kuhn.** 1998. Interaction of *Listeria monocytogenes* with human brain microvascular endothelial cells: InlB-dependent invasion, long-term intracellular growth, and spread from macrophages to endothelial cells. Infect. Immun. **66:**5260–5267.
18. **Hakim, J. G., I. T. Gangaidzo, R. S. Heyderman, J. Mielke, E. Mushangi, A. Taziwa, V. J. Robertson, P. Musvaire, and P. R. Mason.** 2000. Impact of HIV infection on meningitis in Harare, Zimbabwe: a prospective study of 406 predominantly adult patients. AIDS **14:**1401–1407.
19. **Huang, S. H., C. Wass, Q. Fu, N. V. Prasadarao, M. Stins, and K. S. Kim.** 1995. *Escherichia coli* invasion of brain microvascular endothelial cells in vitro and in vivo: molecular cloning and characterization of invasion gene *ibe10*. Infect. Immun. **63:**4470–4475.
20. **Ibrahim, A. S., S. G. Filler, M. S. Alcouloumre, T. R. Kozel, J. E. J. Edwards, and M. A. Ghannoum.** 1995. Adherence to and damage of endothelial cells by *Cryptococcus neoformans* in vitro: role of the capsule. Infect. Immun. **63:**4368–4374.
21. **Jaffe, E. A., L. W. Hoyer, and R. L. Nachman.** 1973. Synthesis of antihemophilic factor by cultured endothelial cells. J. Clin. Investig. **52:**2757–2764.
22. **Jong, A. Y., M. F. Stins, S.-H. Huang, S. H. M. Chen, and K. S. Kim.** 2001. Traversal of *Candida albicans* across human blood-brain barrier in vitro. Infect. Immun. **69:**4536–4544.
23. **Kim, K. S.** 2000. *E. coli* invasion of brain microvascular endothelial cells as a pathogenetic basis of meningitis. Subcell. Biochem. **33:**47–59.
24. **Kim, K. S.** 2003. Pathogenesis of bacterial meningitis: from bacteria to neuronal injury. Nat. Rev. Neurosci. **4:**376–385.
25. **Kwon-Chung, K. J., and J. E. Bennett.** 1992. Medical mycology. Lea & Febiger, Philadelphia, Pa.
26. **Lane, J. H., V. G. Sasseville, M. O. Smith, P. Vogel, D. R. Pauley, M. P. Heyes, and A. A. Lackner.** 1996. Neuroinvasion by simian immunodeficiency virus coincides with increased numbers of perivascular macrophages/microglia and intrathecal immune activation. J. Neurovirol. **2:**423–432.
27. **Lonsdale-Eccles, J. D., and D. J. Grab.** 2002. Trypanosome hydrolases and the blood-brain barrier. Trends Parasitol. **18:**17–19.
28. **McCaffery, J. M., and M. G. Farquhar.** 1995. Localization of GTPases (GTP-binding proteins) by indirect immunofluorescence and immunoelectron microscopy. Methods Enzymol. **257:**259–279.
29. **Merkel, G., and B. A. Scofield.** 1997. The in vitro interaction of *Cryptococcus neoformans* with primary rat lung cell cultures. FEMS Immunol. Med. Microbiol. **19:**203–213.
30. **Merkel, G. J., and B. A. Scofield.** 1994. Comparisons between in vitro glial cell adherence and internalization of non-encapsulated and encapsulated strains of *Cryptococcus neoformans*. J. Med. Vet. Mycol. **32:**361–372.
31. **Nizet, V., K. S. Kim, M. Stins, M. Jonas, E. Y. Chi, D. Nguyen, and C. E. Rubens.** 1997. Invasion of brain microvascular endothelial cells by group B streptococci. Infect. Immun. **65:**5074–5081.
32. **Pardridge, W. M.** 1999. Blood-brain barrier biology and methodology. J. Neurovirol. **5:**556–569.
33. **Paspalas, C. D., and G. C. Papadopoulos.** 1996. Ultrastructural relationships between noradrenergic nerve fibers and non-neural elements in the rat cerebral cortex. Glia **17:**133–146.
34. **Prasadarao, N. A., C. A. Wass, M. F. Stins, H. Shimada, and K. S. Kim.** 1999. Outer membrane protein A-promoted actin condensation of brain microvasucular endothelial cells is required for *Escherichia coli* invasion. Infect. Immun. **67:**5775–5783.
35. **Prockop, L. D., and K. A. Naidu.** 1997. Entry rate kinetics of D-mannitol and carboxy-inulin for transfer across the blood-cerebrospinal fluid barrier. J. Spinal Cord Med. **20:**391–394.
36. **Pujol, C., E. Eugene, L. de Saint Martin, and X. Nassif.** 1997. Interaction of *Neisseria meningitidis* with a polarized monolayer of epithelial cells. Infect. Immun. **65:**4836–4842.
37. **Ring, A., J. N. Weiser, and E. I. Tuomanen.** 1998. Pneumococcal trafficking across the blood-brain barrier. J. Clin. Investig. **102:**347–360.
38. **Rubin, L. L.** 1999. The cell biology of the blood-brain barrier. Annu. Rev. Neurosci. **22:**11–28.
39. **Santangelo, R., H. Zoellner, T. Sorrell, C. Wilson, C. Donald, J. Djordjevic, Y. Shounan, and L. Wright.** 2004. Role of extracellular phospholipases and mononuclear phagocytes in dissemination of cryptococcosis in a murine model. Infect. Immun. **72:**2229–2239.
40. **Stins, M. F., J. Badger, and K. S. Kim.** 2001. Bacterial invasion and transcytosis in transfected human brain microvascular endothelial cells. Microb. Pathog. **30:**19–28.
41. **Stins, M. F., F. Gilles, and K. S. Kim.** 1997. Selective expression of adhesion molecules on human brain microvascular endothelial cells. J. Neuroimmunol. **76:**81–90.
42. **Stins, M. F., Y. Shen, S. H. Huang, F. Gilles, V. K. Kalra, and K. S. Kim.** 2001. Gp120 activates children's brain endothelial cells via CD4. J. Neurovirol. **7:**125–134.

*Editor:* T. R. Kozel